Canadian Mineralogist
Vol. 15, pp. 446-458 (1977)

AN IDEALIZED MODEL FOR SERPENTINE TEXTURES AFTER OLIVINE

F. J. WICKS[1], E. J. W. WHITTAKER, AND J. ZUSSMAN[2]
University of Oxford, Department of Geology and Mineralogy, Parks Road, Oxford OX1 3PR, England

Abstract

Olivine is well-known to alter to serpentine with a characteristic mesh or hourglass texture. Various two-dimensional classifications of the textures have previously been developed, with some explanation in three-dimensional terms, but an extensive three-dimensional model explains more features.

A fractured olivine crystal is represented ideally as an orthogonally stacked assemblage of identical cubes. Apparent serpentine fibers are imagined developing simultaneously normal to all cube faces at a uniform rate, and either (1) developing until all the olivine is gone, (2) replacing the olivine only half-way in from the surface, and (3) subsequently replacing the olivine left in (2) by randomly oriented fine-grained serpentine. Sections are taken so that the normal to the plane of the section lies along various directions relative to the symmetry elements of the cube. Case 1 produces hourglass textures with minor mesh textures; case 2 produces mesh textures, mainly with olivine mesh centers and some minor hourglass textures; case 3 produces mesh textures, mainly with isotropic mesh centers and some minor hourglass textures. Although these idealized textures cannot be expected to correspond directly to observed textures, they lead to an understanding and possible explanation of many of the observed textures, and show the importance of the third dimension in thin-section studies of serpentine textures.

Sommaire

C'est bien connu, l'olivine se transforme en serpentine avec une texture maillée ou en sablier qui lui est propre. On a déjà élaboré différentes sortes de textures en deux dimensions, accompagnées d'explications en termes tridimensionnels, mais une maquette permet de définir plusieurs autres traits.

Un cristal d'olivine fracturé est représenté, de façon idéale, par un empilement orthogonal de cubes identiques. Les fibres apparentes de serpentine semblent se développer simultanément, normals à toutes les faces du cube à une vitesse uniforme, et soit (1) se développant jusqu'à ce qu'il n'y ait plus d'olivine, (2) en remplaçant l'olivine jusqu'à mi-chemin de la surface et (3) par remplacement subséquent de l'olivine qui restait en (2) par de la serpentine à grains fins sans orientation spécifique. Des sections ont été choisies de façon à ce que l'orientation de la normal au plan de la section soit dans plusieurs directions relatives aux éléments de symétrie du cube. Le premier cas, produit des textures en sablier accompagnées de petites textures maillées; le deuxième cas produit des textures maillées contenant principalement des centres maillés d'olivine et de petites textures en sablier; enfin le troisième cas produit des textures maillées avec, principalement, des centres maillés isotropiques et quelques petites textures en sablier. Bien que ces textures idéalisées ne peuvent correspondre directement aux textures observées, elles nous aident à comprendre et à expliquer les diverses textures observées, et elles démontrent l'importance de la troisième dimension dans les études en lames minces des textures de serpentine.

(Traduit par la Rédaction)

Present address:
[1]Department of Mineralogy and Geology, Royal Ontario Museum, Toronto, Canada.
[2]Department of Geology, The University, Manchester, England.

Introduction

Serpentine pseudomorphs after olivine have long been recognized in thin section by their characteristic mesh and hourglass textures. Either an idealized square or rectilinear model has been used for the description of these textures (Selfridge 1936; Francis 1956; Deer *et al.* 1962; Klinkhammer & Rost 1967), or else a more realistically shaped, irregular model (Tertsch 1922; Klinkhammer 1962; Klinkhammer & Rost 1967; Coats 1968). Although these two-dimensional models are descriptively useful, it must be remembered that textures are three-dimensional structures which we happen to study two-dimensionally through the use of thin sections, and only Selfridge (1936) and Klinkhammer (1962) have made a limited study of the effect of the third dimension. It is difficult to appreciate fully the third dimension in normal thin-section studies, and such an appreciation is made even more difficult if a two-dimensional rectilinear model is used, as this subtly forces the observer to forget the effect of the third dimension and to interpret all features in two-dimensional terms. Although no idealized three-dimensional model will reproduce the exact textures in thin sections, such a model leads to a much clearer insight into the nature and inter-relationships of the textures observed. It is the purpose of this paper to develop and analyze such a three-dimensional model.

Previous Studies and Current Terminology

Olivine readily alters to serpentine along grain boundaries and fractures to produce a characteristic texture which in thin section appears as an irregular tessellation of polygonal cells. Each cell has a central zone composed of relict olivine (Fig. 1a) or of serpentine (Fig. 1b). An outer zone of apparently fibrous serpentine surrounds the central zone and is itself surrounded by the site of the original fractures or grain boundaries. The apparent fiber axes of the serpentine of the outer zone are aligned approximately at right angles to the trace of the original fracture. On the other side of the site of the fracture, the sequence is repeated in reverse into the central zone of the next cell. In this paper we will call this assemblage of cells mesh texture, the central zone of each cell a mesh center, the outer zone a mesh rim, and the site of the original fracture the central parting of the mesh rim. The term mesh rim usually includes the outer zone of adjacent cells on either side of the central parting (Fig. 1a). In previous descriptions the mesh rim has been called a vein by du Rietz (1935) and Selfridge (1936); a ribbon or band (Bänd) by Tertsch (1922), Angel (1930) and many others; a frame, framework or common framework fiber (Rahmen, gemeine Rahmenfaser) by Angel (1930), Rost (1959), Klinkhammer (1962) and Hochstetter (1965); a collar by Francis (1956); or mesh wall, chrysotile wall (Maschenwand, Chrysotilwand) by Angel (1964), to mention only a few. The mesh center has been called a field (Feld) by Tertsch (1922); a mesh field (Maschenfeld) by Gees (1956); an inner field (Innenfeld) by Klinkhammer (1962) and Hochstetter (1965); or a core by Francis (1956), Deer *et al.* (1962) and Grubb (1962).

In the series of mesh textures studied in detail by Wicks & Whittaker (1977) in association with this study, the mesh rims were found to range from 0.01 to 0.30 mm wide and average 0.07 mm. The mesh cells examined range from 0.05 to 0.56 mm across from parting to parting, and average 0.27 mm.

The descriptive classification of these textures has evolved through the work of Tertsch (1922), Angel (1930), du Rietz (1935), Selfridge (1936), Francis (1956), Gees (1956), Rost (1959), Deer *et al.* (1962), Klinkhammer (1962), Hochstetter (1965) and Tröger (1969). In this classification, the serpentine minerals are distinguished by the optical characteristics along the apparent fiber axis: length-fast apparent fibers (negative elongation) are called α-serpentine and length-slow apparent fibers (positive elongation) are called γ-serpentine (Tertsch 1922). Because of the apparently fibrous character of these materials, the terms chrysotile-α and chrysotile-γ (Chrysotil-α and Chrysotil-γ, Gees 1956; Tröger 1969) and X-fiber and Z-fiber (X-Faser and Z-Faser, Rost 1959; Tröger 1969) have been used. However, this is misleading as Wicks & Zussman (1975) have shown that α-serpentine is usually lizardite and not truly fibrous, and γ-serpentine, can be chrysotile, lizardite, or antigorite, with the last two not being truly fibrous. Therefore, it is recommended that the less specific terms, α-serpentine and γ-serpentine, first proposed by Tertsch (1922), be used.

In Tertsch's (1922) description, two types of textures were distinguished, namely window-structure (Fensterstruktur) with rims of α-serpentine and centers of γ-serpentine, and mesh-structure (Maschenstruktur) with rims of γ-serpentine and centers of α-serpentine. Other terms, such as net-serpentine (Netzserpentin, Gees 1956; Peters 1963) and trellis, or lattice-serpentine (Gitterserpentin), also have been used. The latter term was originally used to describe serpentine after amphibole (Weigand 1875) and pyroxene (Angel 1930), but was later applied to antigorite after serpentine mesh textures (Gees 1956) and serpentine after olivine (du Rietz 1935; Rost 1959). Of these descriptive terms, only mesh texture (Francis 1956) or mesh structure (Deer *et al.* 1962) are in general use in the English literature.

Detailed as Tertsch's descriptions are, anomalies appear when his descriptions are applied to serpentine textures from a large number of localities such as those upon which the present study is based (Wicks & Whittaker 1977). Mesh centers are not uniformly of opposite elongation to the mesh rims, nor indeed are they of any single characteristic type. Although the two types of mesh rims, α-serpentine and γ-serpentine, generally show little variation between samples, mesh centers show a wide variation. Mesh centers can be composed of either or both α- and γ-serpentine apparent fibers, in a single orientation or several orientations, including a regular hourglass configuration (Fig. 1c). The birefringence of the mesh centers varies, but is usually lower than the birefringence of the mesh rims (Fig. 1c). In some cases the mesh centers may show no apparent fiber direction, and may be isotropic (Fig. 1b). The term serpophite was

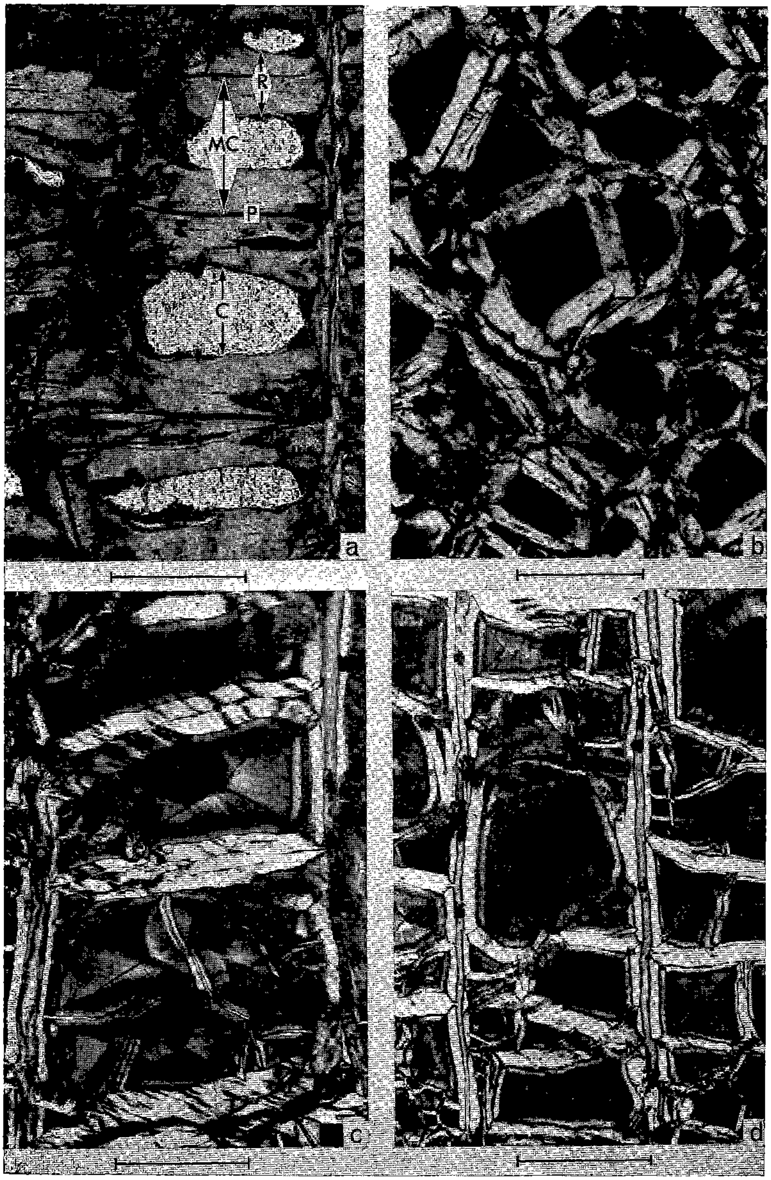

FIG. 1. (a) α-serpentine (lizardite $1T$) mesh texture with olivine mesh centers, C. The mesh rims, R, are composed of α-serpentine and contain a central parting, P, that marks the site of the original fracture in the olivine. A mesh cell, MC, is defined as the volume contained within adjacent partings. Sample IB67-201, Murray Ridge, British Columbia. Compare with Figure 7c, case 2. (b) α-serpentine (lizardite $1T$) and brucite mesh texture with isotropic serpentine (lizardite $1T$) mesh centers. Sample 18508, Glen Urquhart, Scotland. Compare the mesh cells in the top left corner with Figure 6a, case 3. (c) α-serpentine (lizardite $1T$) mesh texture with α-serpentine (lizardite $1T$) hourglass mesh centers. Sample N-111A-2, Normandie mine, Quebec. (d) α-serpentine (lizardite $1T$) mesh texture with the vertical central partings filled with γ-serpentine. Sample N-111A-2. Normandie mine. Compare the case 3 form without the γ-serpentine in the central partings with Figure 5b, case 3. All under crossed nicols. Bar represents 0.2 mm.

proposed by Lodochnikov (1933) to describe such isotropic serpentine, and it has been suggested that it is amorphous, but Wicks & Zussman (1975) have shown it to be composed of randomly oriented fine-grained lizardite 1*T* or, less commonly, of a lizardite plate viewed down the *z* axis. Mesh centers of red-brown "bowlingite" or "iddingsite" have also been observed by Francis (1956) and Mattson (1964), but the mineralogy of these is discussed in Wicks & Whittaker (1977). The development of mesh centers after olivine through several stages of growth, often leading to the development of antigorite, has been described by du Rietz (1935), Gees (1956), and Peters (1963), but as the identifications are based on optical criteria rather than X-ray diffraction criteria, it is not possible to correlate them with the microbeam X-ray camera results.

Because the mesh centers display such a variation, it is best to modify Tertsch's terminology so that mesh textures are characterized solely by the optical orientation of the serpentine in the mesh rims without reference to the optical orientation of the serpentine in the mesh centers. Thus it is recommended that the term α-serpentine mesh texture be used to refer to all mesh textures with mesh rims of α-serpentine, and conversely, γ-serpentine mesh texture be used to refer to all mesh textures with mesh rims of γ-serpentine.

Even though mesh rims usually display less variation than mesh centers, some confusion can arise in defining exactly what makes up a mesh rim. The site of the original fracture in the olivine may be marked as a simple parting (Fig. 1a), or by a string of magnetite grains (Fig. 2d), or by a narrow (sometimes discontinuous) zone of isotropic or anisotropic serpentine (Fig. 1d and du Rietz 1935; Selfridge 1936; Gees 1956). Where this serpentine is anisotropic, it often has a fiber elongation opposite to that of the mesh rim lying on either side of it. If it is very thin it can be ignored and the mesh texture can be characterized by the elongation of the apparent fibers in the main part of the mesh rim. Sometimes it is obviously a later chrysotile vein that has followed a plane of weakness, and again can be ignored in discussion of the mesh textures. Occasionally, however, there appear to be two partings with an intermediate zone between them having the same elongation as the mesh rims to either side. Since Francis (1956) described mesh rims as bipartite veins because the central parting divided them into two parts (Fig. 1a), Coats (1968) suggested the term tripartite veins to describe these rims with two partings (Fig. 2a). Rims containing three partings also occur and have been called compound mesh rims. In these the zone that surrounds the mesh center is itself surrounded by a second zone (of opposite elongation) so that in going from one mesh center to the next, four zones are encountered, two at each side of the original parting (Fig. 2b). These can be called the outer rim, adjacent to the central parting, and the inner rim, adjacent to the mesh center, and are equivalent to the outer framework (Aussenrahmen) and inner framework (Innenrahmen) of Rost (1959), or the complex wall formation (komplexen Wandbau) of Angel (1964). Still greater complexity arises in the rare cases where mesh rims contain more than three partings.

Mesh cells can vary considerably in both size and shape from one thin section to another, and even within a single thin section. Coats (1968) has described mesh textures as symmetric (Fig. 1d) or asymmetric (Fig. 2c) depending on the shape and regularity of the development of individual mesh cells. Francis (1956) used the term banded or curtain-like growth to describe sets of bipartite veins sub-parallel to a single direction so that no distinct mesh structure appears (Fig. 2d). The term Bänder-Serpentinit is used by Klinkhammer (1962), Hochstetter (1965), and Tröger (1969) to describe this feature, although the term Bänder was also used by earlier researchers to describe mesh rims (Tertsch 1922; Gees 1956).

The textures that have commonly been described as hourglass textures or hourglass structures (Tertsch 1922; Angel 1930; Deer *et al.* 1962; Hochstetter 1965; Tröger 1969) have usually been mesh textures having an hourglass mesh center (Fig. 1c). The cross-mesh (Kreuzmaschen) described by Rost (1956), Klinkhammer (1962) and Klinkhammer & Rost (1967) is similar, and a texture formed after pyroxene was also described as hourglass texture by Selfridge (1936). However, there also exists what may be described as a pure hourglass texture in which there are no mesh rims surrounding the "hourglasses". This can be considered as corresponding to a regular mesh texture in which the mesh rims continue inwards until they meet at the grain center, so that no mesh center is present (Fig. 3a). Such textures have been illustrated by Klinkhammer (1962, his Fig. 16), but not discussed. In some pure hourglass textures studied in detail by Wicks & Whittaker (1977) the hourglass cells ranged from 0.12 to 0.60 mm across from parting to parting, with an average of 0.39 mm. These various features and their relationship to one another will be discussed in terms of an idealized three dimensional model.

Wicks & Zussman (1975), by use of a micro-

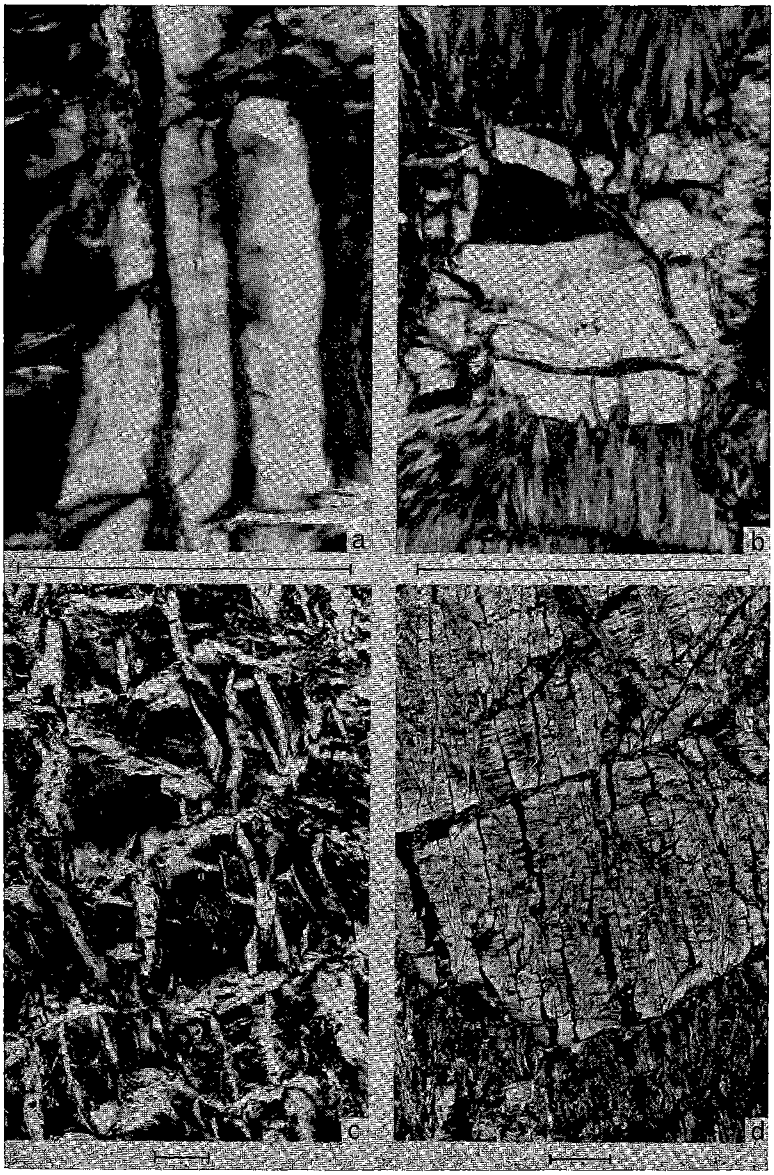

FIG. 2. (a) Tripartite α-serpentine (lizardite $1T$) mesh rim. Sample 18508, Glen Urquhart, Scotland. Compare with Figure 5c, section 3. (b) Mesh texture with compound mesh rims of γ-serpentine (antigorite) adjacent to the central parting, and α-serpentine (lizardite $1T$) between the γ-serpentine zone and the isotropic serpentine (lizardite $1T$) mesh centers. Sample 03-69-284-1, Fox River, Manitoba. (c) γ-serpentine (chrysotile $2M_{c1}$ mesh texture with isotropic serpentine, α-serpentine and γ-serpentine (all intimately associated chrysotile $2M_{c1}$ and lizardite $1T$) in the mesh centers. Sample 18501, Pipe Lake mine, Manitoba. (d) α-serpentine (lizardite $1T$) banded growth or curtain texture. The central partings lie vertically, and in places contain magnetite lenses. The apparent fibers run from left to right. Sample 18506, Setting Lake, Manitoba. Compare with Figure 5c, section 2. All under crossed nicols. Bar represents 0.2 mm.

FIG. 3. (a) γ-serpentine (antigorite) hourglass texture. Sample 18558, Knee Lake, Manitoba. Compare with Figures 5c and 6b, both case 1. (b) α-serpentine (lizardite $1T$) hourglass texture and mesh texture with isotropic serpentine (lizardite $1T$) in the mesh center. Sample AG67-35b, Jeffrey mine, Quebec. Compare with Figure 5a, section 2. All under crossed nicols. Bar represents 0.2 mm.

beam X-ray diffraction camera, have shown that α-serpentine mesh and hourglass textures are composed of lizardite $1T$, whereas γ-serpentine mesh and hourglass textures may be composed of antigorite, chrysotile, or lizardite $1T$. They also found that the serpentine in many of these textures is only "apparently fibrous", chrysotile alone being truly fibrous. Further mineralogical details are discussed in Wicks & Whittaker (1977).

An Idealized Three-Dimensional Model

The simplest three-dimensional model of a fractured olivine crystal is an assemblage of orthogonally stacked identical cubes, each of which represents a fracture fragment of the crystal. Serpentine can be imagined developing at right angles to, and simultaneously on, each cube face, replacing olivine at a uniform rate and at a constant volume. The serpentine is assumed to be either fibrous, or "apparently fibrous", with the fibers at right angles to the cube faces. The serpentine developing inward from any given cube face will be limited by that developing inward from the four adjacent cube faces. If the serpentinization continues uniformly until all the olivine is replaced, the intersection of the boundaries between the serpentine developed inward from each cube face will be the body-center of the cube. This type of serpentinization will be called case 1 (Fig. 5a). It is also possible that the serpentinization of the olivine will stop, leaving a central core of unaltered olivine (case 2, Fig. 5a). Such a central core may then conceivably be replaced by serpentine in a subsequent episode. If the material so produced is a mass of randomly oriented fine-grained serpentine, the situation will be called case 3 (Fig. 5a). It is also possible, of course, that in the subsequent episode the core will be replaced by oriented serpentine just as the whole cube was in case 1. This possibility is not illustrated separately, as it may be readily visualized as an insertion of the appropriate diagrams of case 1 into the cores of case 2. There are many other combinations that could be proposed, but the three cases defined above provide sufficient variation for the purposes of this discussion.

It may be assumed that the randomly oriented serpentine in the central zone in case 3 will appear isotropic. The parallel "apparent fibers" developed in from the cube faces will display their greatest birefringence in sections that cut them parallel to the fiber axis and they will be isotropic in sections at right angles to the fiber

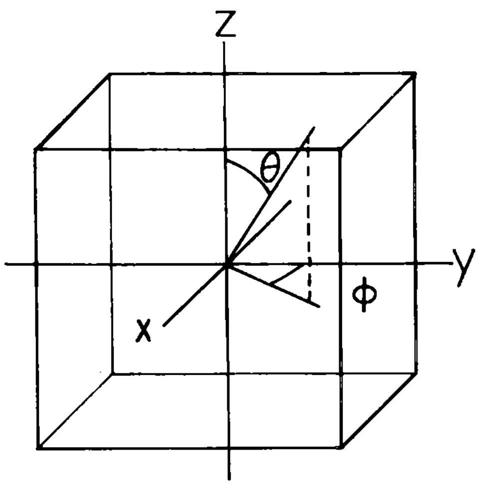

FIG. 4. Coordinate axes and angular coordinates located with respect to an idealized unit cube of olivine imagined to be bounded by fracture planes from which serpentine may proceed inwards.

axis. In the latter position the serpentine will appear to be featureless, but in all sections where the angle between the section and the "apparent fiber" axis is not near 90° the serpentine will appear to be fibrous and have intermediate birefringence. Thus in this model, isotropic serpentine can be either randomly oriented serpentine or parallel "apparent fibers" seen end-on, and there is no optical criterion to distinguish which type is present in any given section.

The various different two-dimensional textures that may be expected in thin sections of idealized models of the above three cases may be analyzed in terms of the orientation of the plane of the section to the edges of the cubes, and it is assumed that the thickness of the thin section is small compared with the size of the cube, so that it can be approximated by a mathematical plane. This is usually justified since the section is 30 μm thick and the average cell size is about ten times as great. A system of mutually perpendicular axes x, y and z is chosen parallel to the cube edges, with the origin of the system at the body-center of one cube (Fig. 4). Any plane that passes through the cube can then be defined in terms of its distance from the origin and of the angles θ and ϕ, where θ is the angle between z and the normal to the plane, and ϕ is the angle between y and the projection of the normal on the xy plane (Fig. 4). Because of the symmetry of the cube, only one octant need be examined. Different kinds of sections are obtained depending on the direction of the section normal with respect to the various symmetry elements of the cube; to ensure that all kinds of sections are considered, the normal is placed on each symmetry element in turn, and finally in a general orientation.

The series of sections illustrated in Figures 5 to 7 were developed by descriptive geometry. Each section is defined in terms of θ and ϕ, and by the symmetry element (if any) on which the section normal lies. The heavy lines in the drawings represent the site of the original fractures in the olivine, and thin lines represent boundaries between serpentine in different orientations, or between serpentine and olivine. The shapes of the textural units, bounded by the heavy lines, reflect the symmetry of the symmetry element with which the section normal is in coincidence.

The sections that pass through the cube so that the section normal lies along the 4-fold (θ=0°, ϕ indeterminate) or 2-fold axes (θ=45°, ϕ=0°) are characterized by 4-fold symmetry and square outlines, or 2-fold symmetry and rectangular outlines, respectively (Figs. 5a and c). These are, in fact, the kinds of diagrams most frequently used to depict mesh and hourglass textures (Francis 1956; Deer *et al.* 1962). Similarly, a section with its normal along the 3-fold axis (θ=54°44′, ϕ=45°) has 3-fold symmetry and equilateral triangles alone (section 1), or regular hexagons and equilateral triangles (section 3), or a mixture of two sizes of equilateral

FIGS. 5-7. The appearances expected in sections at different distances from the origin are necessarily shown in separate diagrams, although in practice the random sizes of fracture cells will lead to their being mixed within a given specimen. For convenience of drawing, the appearances expected from the three types of serpentinization are combined in each diagram, although in practice these will tend to occur in different specimens. The heavy lines represent the sites of fractures in the original olivine, and the thin lines represent boundaries between serpentine in different orientations, or between serpentine and olivine. Sections normal to symmetry axes of the cube (Figs. 5a, 5c and 6c) give rise to qualitatively different appearances, depending on their distances from the origin, and two or three different sections are therefore shown. In other cases, the section cuts successive cells at different distances from the origin, and the various possible appearances develop (and are shown) successively along one section. In all such cases, the direction through successive cells of one case is indicated by the arrow adjacent to the case label. Some sections perpendicular to the 3-fold axis of the cube have features in common among the three cases, and in Figure 6c these are not drawn separately, so that some parts of these diagrams belong to the sequence of appearances belonging to different cases.

triangles and hexagons with two unequal sets of edges (section 2) depending on the distance of the section from the origin (Fig. 6c).

When the section normal lies on the axial mirror plane, the textural units have rectangular outlines and bilateral symmetry (Fig. 5b), and are intermediate between the sections at the 4-fold axis and the 2-fold axis. The textures in sec-

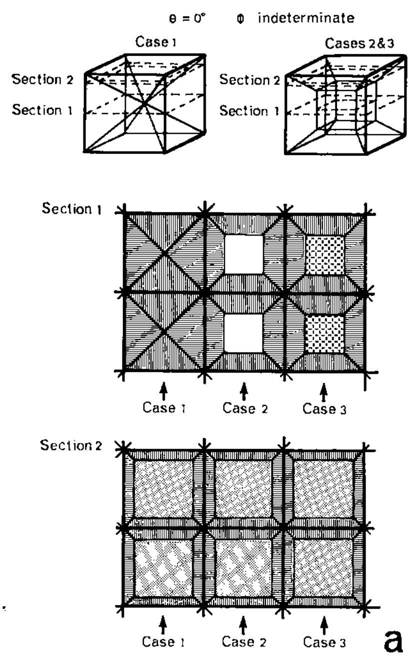

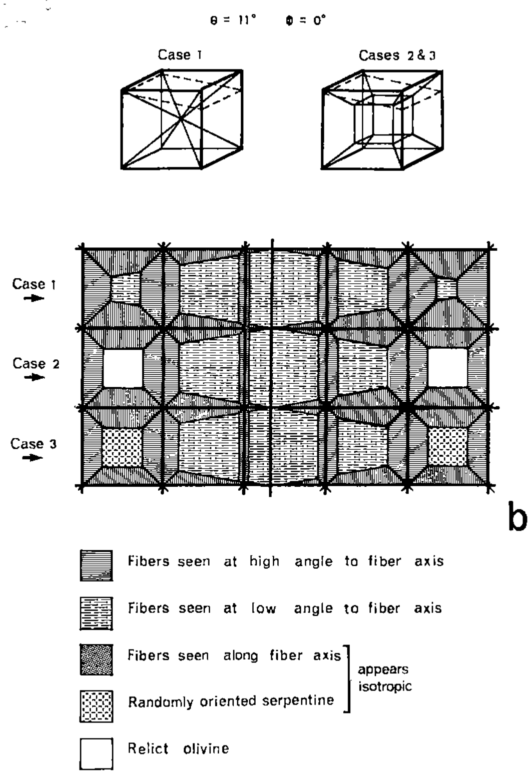

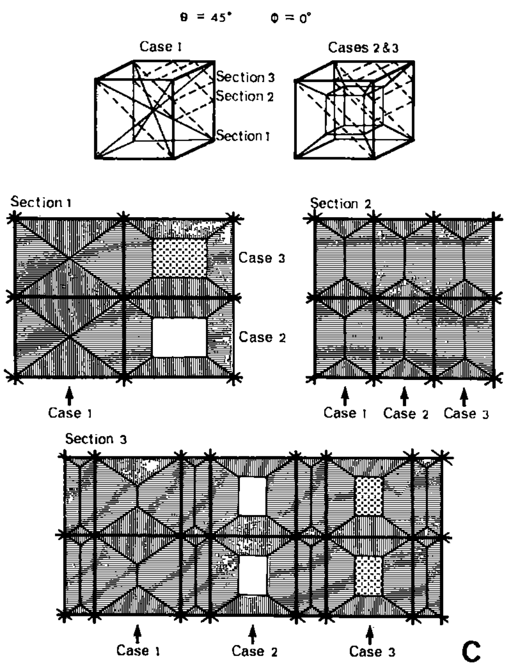

FIG. 5. (a) Section with normal along the 4-fold axis. $\theta=0°$, ϕ indeterminate. (b) Section with normal on the axial mirror plane, and lying between the 4-fold and 2-fold axes. $\theta=11°$, $\phi=0°$. (c) Section with normal along the 2-fold axis. $\theta=45°$, $\phi=0°$.

tions whose normal lies on the diagonal mirror plane are more complex. If the normal lies between the 4-fold and the 3-fold rotation axes, the textural units are characterized by isosceles triangles with each of the two equal sides shorter than the third side, and by rhombs and pentagons – all with bilateral symmetry (Figs. 7a and b). Those that lie between the 3-fold and 2-fold rotation axes are characterized by isosceles triangles with each of the two equal sides longer than the third side, trapezia and irregular hexagons with bilateral symmetry (Figs. 6a and b).

The only other texture that can be developed is one in which the section normal does not lie on a symmetry element. This texture is characterized by scalene triangles, rhombs, trapezia, and irregular pentagons and hexagons – with no symmetry (Fig. 7c).

Two types of textures, mesh and pure hourglass, are present in these sections. However, case 1, which might be intuitively associated

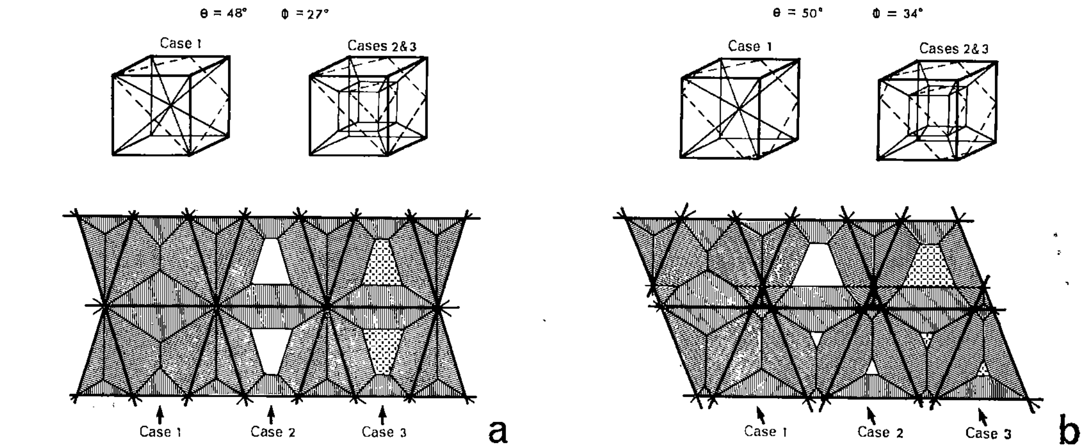

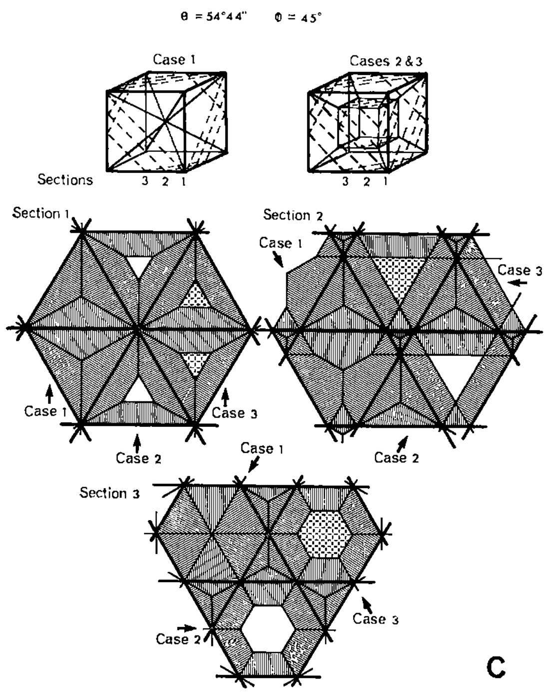

FIG. 6. Sections with normals on the diagonal mirror plane, and lying between the 2-fold and 3-fold axes. (a) at $\theta=48°$, $\phi=27°$ and (b) at $\theta=50°$, $\phi=34°$. (c) Section with normal along the 3-fold axis. $\theta=54°44'$, $\phi=45°$.

with pure hourglass texture, does not always produce this texture. Mesh textures are produced in most sections in which the section normal lies along a 4-fold axis (Fig. 5a, section 2) or nearly so (Figs. 5b and 7b). Conversely, although case 2 or case 3 might be expected to be associated with mesh texture, each can in fact produce a limited amount of pure hourglass texture in sections in which the normal is along a 2-fold axis (Fig. 5c, section 2) or nearly so (Fig. 7c). In classifying textures as mesh or pure hourglass, the many smaller triangular configurations that occur in both textures have been disregarded.

In order to estimate the frequency of occurrence of these two types of texture produced in the three cases, it is necessary to decide over what range, measured as the angle (α) of divergence of the section normal from a given symmetry element, any given textural shape will be recognizable before giving way to another shape. An arbitrary value of α of 5° was chosen for purposes of calculation.

If a sphere, with a diameter equal to the cube edge, is imagined lying within the cube so that the center of the sphere is at the body-center of the cube, each of the textural shapes related to the rotation axes will occur with a frequency proportional to the area of a circle, of radius α, on the surface of the sphere. Similarly, the textural shapes related to the planes of symmetry will be represented by the area of a zone, of half width α, about the trace of the mirror plane, less the areas of the circles representing the rotation axes. Other textural shapes whose section normals do not lie on symmetry elements will be represented by the area of the surface of the

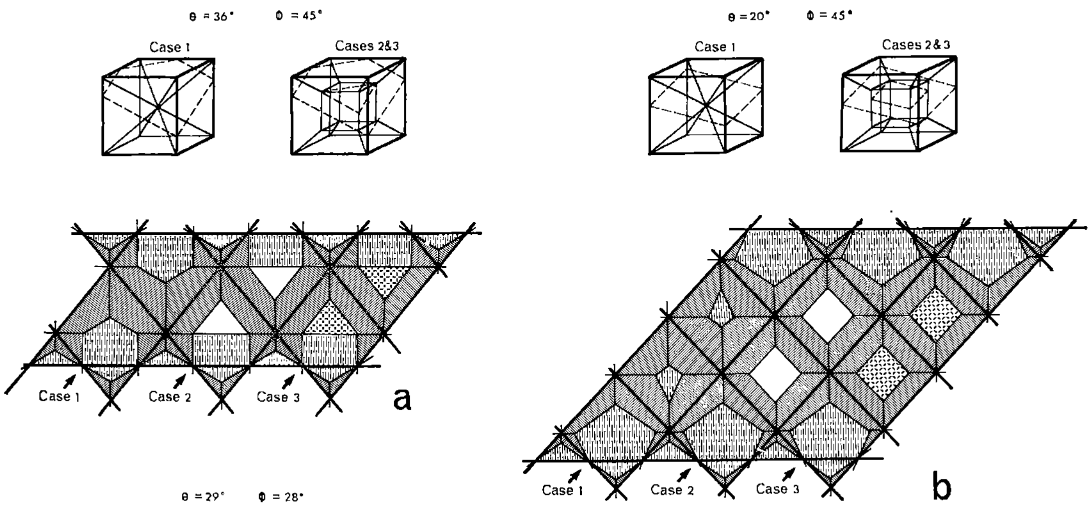

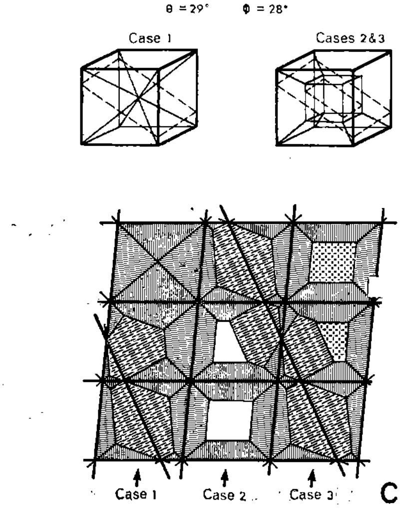

FIG. 7. Sections with normals on the diagonal mirror plane, and lying between the 3-fold and 4-fold axes. (a) at $\theta=36°$, $\phi=45°$ and (b) at $\theta=20°$, $\phi=45°$. (c) Section in general orientation. $\theta=29°$, $\phi=28°$.

TABLE 1. PERCENTAGES OF THE VARIOUS TEXTURES

Symmetry element containing the section normal	Fig. No.	Tolerance % at 5°	Main Texture Type Case 1	Case 2	Case 3
4-axis	5a	1.1	mesh and minor hourglass	mesh	mesh
3-axis	6c	1.5	hourglass	mesh and some hourglass	mesh and some hourglass
2-axis	5c	2.3	hourglass	mesh and some hourglass	mesh and some hourglass
axial m-plane (between 4- and 2-axes)	5b	19.5	mesh	mesh	mesh
diagonal m-plane (between 2- and 3-axes)	6a, 6b	14.4	hourglass	mesh	mesh
diagonal m-plane (between 4- and 3-axes)	7a, 7b	24.2	hourglass and mesh	mesh and some hourglass	mesh and some hourglass
1	7c	37.0	hourglass	mesh and some hourglass	mesh and some hourglass

remainder of the sphere. Because of the symmetry of the cube, only the surface of the sphere lying within an octant of the cube need be examined.

The results (Table 1) show that textural shapes corresponding to the section normals lying along the symmetry axes of the cube will occur very infrequently. The textural shapes corresponding to the section normals lying along the mirror planes occur with reasonable frequency, but the textural shapes whose section normals do not correspond to any symmetry element occur with the greatest frequency. Knowing the frequency of occurrence of the various ideal textural shapes, it is possible to see what effect is expected from the three different cases of serpentine growth on the development of mesh and pure hourglass textures.

The case 1 alteration (uninterrupted serpentine growth from cube face to body-center) produces pure hourglass textures with subordinate mesh textures in some sections (Figs. 5a and b, 7b). Case 2 alteration (relict olivine core) produces mesh texture with mesh centers formed mainly of olivine, but with some of them formed of serpentine with variable birefringence (Fig. 5b). Only a very few mesh centers have isotropic serpentine (Fig. 5a). Pure hourglass textures are present in some sections (Figs. 5c, and 7b, c), but are not plentiful. Case 3 alteration (random serpentine core) produces results similar to case 2, but with isotropic serpentine mesh centers instead of olivine.

Discussion and Conclusions

Although the results from the idealized cube model cannot be applied directly to an observed texture, they can be used as a basis for interpreting the observed features. A comparison of the photomicrographs in Figures 1, 2 and 3 with the idealized textures in Figures 5, 6 and 7 shows that actual textures can be found that resemble the idealized ones, although the long-range repetition of the idealized textures over many textural units does not occur in nature, of course, because the fractures in the olivine are not likely to occur either at regular intervals, or at equal intervals on the different fracture planes.

The mesh rims in the idealized textures are commonly bipartite as described by Francis (1956). Figure 5c, section 3, offers an explanation for the tripartite mesh rims noted by Coats (1968), and Figure 5c, section 2, offers an explanation for multipartite rims. The various sections through the idealized model show that both symmetrical textural units (Figs. 5, 6, 7a and 7b) and asymmetrical textural units (Fig. 7c) are formed even if the starting form is a cube. Thus, both the symmetrical and asymmetrical mesh cells noted by Coats (1968) can be expected. Any variation away from the cube model would produce even more asymmetrical mesh cells, so that asymmetrical mesh cells can be expected as the rule and the highly symmetrical mesh cells as the exception.

Francis (1956) attributed the development of banded or curtain growth of α-serpentine (Fig. 2d) to shearing during or after serpentinization, but there is another possible explanation. The textures developed when the section normal lies on the 2-fold rotation axis (Fig. 5c, section 2) are similar to the banded growth or curtain-like textures observed by Francis (1956). A rectangular olivine model would develop more convincing banded growth, but if growth of serpentine was limited to two pairs of cube faces instead of all three pairs, then most of the idealized sections would show a form of banded growth. Thus, banded growth and curtain-like textures may reflect the fracture pattern of the olivine and thus the structural environment of the olivine before, rather than during or after, serpentinization.

Consideration of the theoretical textures helps to explain a difficulty encountered in microbeam-camera studies of lizardite mesh textures. A pattern of lizardite with its crystallographic z axis parallel to the X-ray microbeam was not recorded in more than one hundred exposures of mesh centers in the earlier part of the work (Wicks & Zussman 1975). In terms of the idealized model, lizardite plates develop on the cube faces with their crystallographic z axis parallel to the 4-fold axis, and a mesh center of section 2, Figure 5a, in any of the three cases should therefore give an X-ray pattern of this type. Table 1 illustrates the absolute rarity of sections perpendicular to the 4-fold axis, and explains why a substantial number of specimens had been investigated for such sections without success. The difficulty really arose from the fact that those sections had been chosen for investigation from specimens exhibiting many isotropic serpentine mesh centers (Fig. 1b). These were inevitably of case 3, and therefore only a minority of those selected would, in fact, consist of lizardite in the orientation sought. By transferring attention to samples of case 2 with many olivine centers, any isotropic serpentine mesh center should be of the required type (Fig. 5a, section 2), and when this was done an example was soon found (Fig. 3b).

Thus, although the idealized textures cannot be expected to duplicate those found in nature, they provide illumination as to the nature, and inter-relationship, of features that are actually observed.

ACKNOWLEDGEMENTS

We thank Mr. Philip Jackson for his painstaking care and patience in the drafting of the idealized textures, and thank the Royal Ontario Museum Photography Department for photographing them. Our special thanks are extended to Miss Helen Driver and Mrs. Josephine Galt, of ROM, and Mrs. Patricia Moss, of Oxford University, for their efforts in typing the manuscript.

We are grateful to Dr. T. N. Irvine, Geophysical Laboratory, and Dr. R. F. J. Scoates, Manitoba Mines Branch, for supplying some of the specimens, and to Asbestos Corporation, Canadian Johns-Manville Co. Ltd. and Falconbridge Nickel Mines Ltd. for allowing one of us (FJW) to visit and collect specimens at their properties.

REFERENCES

ANGEL, F. (1930): Stubachit und Stubachitserpentin vom Ganoz. *Z. Krist.* 72, 1-41.

——— (1964): Petrographische Studie an der Ultramafit-Masse von Kraubath (Steiermark). *Joanneum Mineral. Mitt.* 2, 1-123.

COATS, C. J. A. (1968): Serpentine minerals from Manitoba. *Can. Mineral.* 9, 321-347.

DEER, W. A., HOWIE, R. A. & ZUSSMAN, J. (1962): *Rock-Forming Minerals* 3. Longmans, London.

DU RIETZ, T. (1935): Peridotites, serpentines and soapstones of northern Sweden. *Geol. Fören. Stockholm Förh.* 57, 133-260.

FRANCIS, G. H. (1956): The serpentinite mass in Glen Urquhart, Inverness-shire, Scotland. *Amer. J. Sci.* 254, 201-226.

GEES, R. A. (1956): Ein Beitrag zum Ophiolith-Problem behandlet an einigen Beispielen aus dem Gebeit von Klosters-Davos (Graubünden). *Schweiz. Mineral. Petrog. Mitt.* 36, 454-488.

GRUBB, P. L. C. (1962): Serpentinization and chrysotile formation in the Matheson ultrabasic belt, northern Ontario. *Econ. Geol.* 57, 1228-1246.

HOCHSTETTER, R. (1965): *Zur Kenntnis der Serpentinmineralien.* Ph.D. thesis, Univ. des Saarlandes.

KLINKHAMMER, B. F. (1962): *Ultrabasite des Ostbayrischen Grenzgebirges.* Ph.D. thesis, Univ. des Saarlandes.

——— & ROST, F. (1967): Die Serpentinite des Oberpfälzer Waldes. *VFMG* 16, 113-136.

LODOCHNIKOV, W. N. (1933): Serpentines and serpentinites and the petrological problems connected with them. *Problems Soviet Geoel.* 2, 145-150.

MATTSON, P. H. (1964): Petrography and structure of serpentinite from Mayaguez, Puerto Rico. *NAS-NRC Publ.* 1188, 7-24.

PETERS, TJ. (1963): Mineralogie und Petrographie des Totalpserpentins bei Davos. *Schweiz. Mineral. Petrog. Mitt.* 43, 529-685.

ROST, F. (1956): Ultrabasische Gesteine in der Münchberger Gneismasse. *Geol. Bavarica* 27, 175-231.

——— (1959): Probleme ultrabasischer Gesteine und ihrer Lagerstätten. *Freiberger Forschungsh.* C-58, 28-65.

SELFRIDGE, G. C. (1936): An X-ray and optical investigation of the serpentine minerals. *Amer. Mineral.* 21, 463-503.

TERTSCH, R. (1922): Studien am Westrande des Dunkelsteiner Granulitmassives. *Tschermaks Mineral. Petrog. Mitt.* 35, 177-214.

TRÖGER, W. E. (1969): *Optische Bestimmung der gesteinsbildenden Minerale.* Teil 2, E. Schweizerbart, Stuttgart.

WEIGAND, B. (1875): Die Serpentine der Vogesen. *Tschermaks Mineral. Petrog. Mitt.* 3, 183-206.

WICKS, F. J. & WHITTAKER, E. J. W. (1977): Serpentine textures and serpentinization. *Can. Mineral.* 15, 459-488.

——— & ZUSSMAN, J. (1975): Microbeam X-ray diffraction patterns of the serpentine minerals. *Can. Mineral.* 13, 244-258.

Received June 1976; revised manuscript accepted May 1977.